Ionics (2015) 21:3097–3107
DOI 10.1007/s11581-015-1495-y

ORIGINAL PAPER

Phosphoric acid functional UV-cured proton conducting polymer membranes for fuel cells

Mustafa Hulusi Uğur[1] · **Nilhan Kayaman-Apohan**[1] · **Duygu Avci**[2] · **Atilla Güngör**[1]

Received: 2 June 2014 / Revised: 19 June 2015 / Accepted: 22 June 2015 / Published online: 15 July 2015

Abstract This paper reports the preparation and characterization of 10-methacryloyloxydecyl-dihydrogenphosphate (MDP)-based UV-curable proton-conducting polymer membranes (UVcPMs). Poly(ethylene glycol diacrylate) (PEGDA), as cross-linking agent, and *N*-vinyl-2-pyrrolidone (NVP), as reactive diluent, were used to arrange the mechanical and physical properties of the resulting membrane. The membrane formulation polymerized under UV irradiation and membranes were characterized by using Fourier transform infrared (FT-IR), thermal gravimetric analysis (TGA) and electrochemical impedans spectroscopy (EIS). The water uptakes, the volume swelling ratio and ion exchange capacity (IEC) measurement of the membranes were performed. The IEC values increase with an increase in MDP monomer content. Proton conductivities were measured as a function of the weight fraction of MDP content of the membrane. The conductivities are of the order of 10^{-4}–10^{-3} Scm^{-1}. The morphology of the membranes was also investigated by Atomic Force Microscopy (AFM). MDP-based UV-cured polymers are first reported as polyelectrolyte membranes.

Keywords Photopolymerization · Conducting polymers · Membranes · Batteries and fuel cells

✉ Nilhan Kayaman-Apohan
napohan@marmara.edu.tr

[1] Department of Chemistry, Marmara University Faculty of Art & Science, Goztepe, 34722 Kadıköy-Istanbul, Turkey

[2] Department of Chemistry, Boğaziçi University, 34342 Bebek-Istanbul, Turkey

Introduction

Proton exchange membrane fuel cells (PEMFCs) are becoming increasingly attractive as choices for alternative power sources in stationary, automotive, and portable applications. They offer many advantages such as high operating efficiency, quiet operation, and environmental friendliness. Commercial PEMFCs such as Nafion®, Acipex®, and Flemion®, which contain sulfonic acid, show high proton conductivity under a wide range of relative humidity (RH) at operating temperature because of well-defined phase separation between the hydrophobic main chains and the hydrophilic side chains [1]. However, they have high cost and limited operation temperature (<80 °C). Therefore, the development of low-cost polymer membranes capable of operating at temperatures above 100 °C at low humidities constitutes a major scientific and engineering challenge [2–4].

To search for an alternative proton-conducting membranes, investigations have focused on the development of acidic or "protogenic" groups which have the ability to facilitate proton conductivity under low-humidity conditions [5]. The polymers carrying phosphonic acid groups are expected to be useful candidates, owing to their high hydrolytic and thermal stability (due to the strength of the C–P bond [6]) and lower methanol permeability and have recently attracted attention as an alternative to sulfonic acid polymers for PEMFCs. They show a higher degree of hydrogen bonding and lower water uptake than their sulfonated analogues at comparable ion exchange capacities (IECs) [7]. Phosphonated polymers have enhanced proton conductivity because of the amphoteric properties provided by phosphonic acid and its high degree of self-dissociation and hydrogen bonding, and the proton is transported through structural diffusion (the Grotthus [8] mechanism) [6, 9–11].

Relatively few studies have been reported on the polymerization of phosphonic acid functionalized monomers. This is mainly due to difficulties in the preparation of polymers with high degrees of phosphonation which is required for high ionic conductivities [12–14] (in either type of polymeric membrane, a high concentration of acids is important to form large hydrogen-bonded aggregates, which provide proton transportation channels [10]). In one such study, Atanasov and Kerres have reported on the synthesis and conductivity of highly phosphonated polypentafluorostyrene. This polymer showed enhanced water attraction with hydration number similar to sulfonated systems, e.g., Nafion [15]. Jannasch and colleagues have recently prepared a series of phosphonated ionic ABA triblock copolymers and studied them as electrolyte membranes. The membranes were found to be phase separated and nanostructured and showed a high thermal stability under air and also showed significantly enhanced proton conductivity [16].

A possible alternative acidic group is phosphoric acid (PA). It shows high proton conductivity (0.568 S cm^{-1} at 150 °C), even in anhydrous form due to its unique proton conduction mechanism by self-ionization and self-dehydration [17]. Therefore, PA and polymer (such as polyacrylamide, Nylon 6-10, polyvinyl alcohol, and polyethylenimine) blends were prepared [18–21]. Protonic conductivity was found to reach values as high as 6.8×10^{-2} S cm^{-1} at 200 °C and 5 % RH with a PA doping level (mole number of PA per repeat unit of PBI) of 5.6 for PA-doped polybenzimidazole membrane [22]. However, high swelling of the membrane up to 200–700 %, depending on the amount of acid, and PA leaching were found to be the main disadvantages of this system.

Molecules with phosphoric acid groups could also be used. For example, it was recently reported that SiO/PEO (polyethylene oxide) containing nanocomposite membranes show good protonic conductivities at temperatures above 100 °C when doped with monododecylphosphate, among a few other acidic moieties. Monododecylphosphate becomes a proton-donating molecule in humid conditions, where the proton dissociates from alkyl-phosphate acid functional groups to form a hydrated proton such as H_3O^+ and $H_5O_2^+$. The proton carrier concentration was found to be proportional to the monododecylphosphate concentration [23, 24].

A polymerizable analog of monododecylphosphate is 10-methacryloyloxydecyl-dihydrogenphosphate (MDP), with a hydrophobic decyl group, an acid group, and the methacrylate functionality giving it polymerizability (Fig. 1) [25, 26]. It has been widely used as a tooth bonding agent in dental adhesives and composite resins [27, 28].

Currently, the dominant technology for polyelectrolyte membrane fabrication is based on thermal polymerization. However, the high cost of synthesis technique, purification of raw materials, and manufacturing of polymers are the major drawbacks. On the other hand, UV-curing is a high-speed, inexpensive, and simple technique widely used in various applications such as inks, coatings, adhesives, dental restoration, and optical devices [29–32]. It also combines advantages such as low-energy consumption and less environmental pollution due to being a solvent-free process. Recently, we reported the preparation of UV-curable sulfonated hybrid membranes. The membranes reached a proton conductivity of 0.138 S cm^{-1} at 50 °C under fully hydrated conditions with very low selectivity toward methanol satisfies the requirements for DMFC applications [33].

In this study, proton-conducting membranes based on MDP, PEGDA, and NVP were prepared by UV-curing via free radical photopolymerization and the membrane properties were investigated. In this system, PEGDA oligomer acted as a cross-linker and also maintained high barrier properties, while MDP was chosen to provide high proton conductivity properties due to its phosphoric acid groups. On the other hand, NVP is a very well-known reactive diluent in UV-curable systems and incorporation to membrane structure pyrrolidone ring improves the membrane performances, such as the mechanical property and the oxidative stability. In addition, MDP monomer is soluble very well in PEGDA and NVP, which are very important criteria to avoid phase separation. This type of architecture allows the combination of a polyelectrolyte major component of a proton-conducting membrane with a cross-linked polymer partner that limits swelling and consequently helps to improve the mechanical properties.

Various properties of the UV-cured membranes such as determination of insoluble part of the cured membranes, water uptake, and volume swelling ratio, IEC, contact angle measurements, TGA, FTIR, AFM, and proton conductivity were investigated in detail.

Experimental

Materials

N-Vinyl-2-pyrrolidone (NVP, ISP-Turkey), poly(ethylene glycol diacrylate) (PEGDA, M_n=258 $gmol^{-1}$, Fluka), and 1-hydroxy-cyclohexylphenyl-ketone (Irgacure-184, Ciba Specialty Chemicals) were used as received. 10-Methacryloyloxydecyl-dihydrogenphosphate (MDP) was kindly provided by Ivoclar Vivadent. Deionized water of 18.2 MΩ cm resistivity obtained from a Milli Q-water purification system (Millipore, Anamed-Turkey) was used.

Preparation of membranes

The membranes based on MDP, NVP, and PEGDA were prepared by UV-curing technique (Fig. 1). UV curing is a

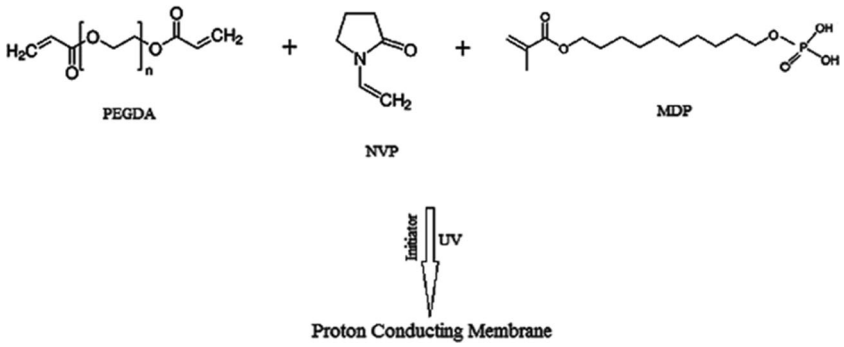

Fig. 1 Reaction scheme for obtaining proton-conducting membranes

conversion process of polymeric materials from a liquid to solid by UV light. All formulations contained 2 wt% of Irgacure-184 as photoinitiator. Before the UV-curing process, the solution was purged with nitrogen gas for 15 min to eliminate dissolved oxygen in the system. Then, the total mixture was transferred to Teflon molds 50 mm×10 mm×1 mm in size. Molecular oxygen can scavenge the free radicals or active radical centers to produce unreactive peroxide radicals. In order to prevent the inhibiting effect of oxygen, the mixture in the mold was covered by transparent 25-μm-thick Teflon film. Finally, the formulations were irradiated for 180 s under UV lamp (OSRAM 300 W, λ_{max}=365 nm). The membranes were removed from the mold and used for further studies. The compositions of membranes are listed in Table 1.

Characterization methods

FTIR spectra were recorded on Perkin Elmer Spectrum 100 ATR-FTIR spectrophotometer

The insoluble part of the UV-cured samples was determined by using a soxhlet extractor, and DMAc was used as solvent. Samples were refluxed in DMAc for 8 h until the sample attained a constant weight. After removal of the solvent by drying at 120 °C for 12 h under vacuum, the remaining mass was weighed as insoluble part. The insoluble and extractable linear part of the UV-cured samples was determined by using (1) and (2) formulas. The residual weights and the initial weights of the UV-cured films are W2 and W1, respectively.

$$\text{Insoluble part}(\%) = W_2/W_1{}^{*}100 \quad (1)$$

$$\text{Soluble part}\ (\%) = (1-W_2/W_1\ )^{*}100 \quad (2)$$

Thermogravimetric analyses (TGA) of the UV-cured membranes were performed using a Perkin-Elmer Thermogravimetric Analyzer Pyris 1 TGA model. Samples were run from 30 to 500 °C with heating rate of 10 °C/min under air atmosphere.

Surface wettability of UV-cured membranes was carried out with a Kruss (Easy Drop DSA-2) tensiometer equipped with a camera. Analyses were made at room temperature by means of the sessile drop technique. For each sample, at least four measurements were made, and the average was taken. The measuring liquid was distilled water.

AFM studies of UV-cured membranes were performed by an Ambios-Quesant Q-Scope Universal Scanning Probe Microscope (SPM) with AFM attachment.

In order to study the water uptake, all of the membranes were first soaked in distilled water at room temperature for 24 h. The swollen membranes were removed from the distilled water, gently wiped with filter paper to remove any water on the surface, and weighed (W_s). All of the swollen membranes were kept under vacuum at 70 °C overnight, after which the dried

Table 1 Composition, codes, conductivity, water uptake, volume swelling ratio, and IEC values of the membranes

Sample	PEGDA (wt%)	NVP (wt%)	MDP (wt%)	MDP/NVP (mole ratio)	Conductivity ($\times10^{-4}$S/cm)	Water uptake (wt.%)	Volume swelling ratio (%)	IEC (mmol H^+/g)
M1	80	10	10	0.34	2.78	36.3	50.7	0.27
M2	70	10	20	0.68	3.89	48.7	72.4	0.37
M3	65	10	25	0.85	4.04	51.5	78.8	0.49
M4	60	10	30	1.00	8.65	70.8	93.4	0.68
M5	50	10	40	1.38	11.1	76.1	116.2	0.84
M6	40	10	50	1.72	6.68	62.8	95.1	0.63

membranes were weighed (W_d). Finally, the water uptake was calculated by using the formula [34]:

$$\text{Water Uptake}\ (\%) = [(W_s - W_d)/W_d] \times 100 \quad (3)$$

All the data reported in this paper are averages of two separate measurements; standard deviations of the measured water uptake were less than 3 % of the mean.

To measure the volume swelling ratio of the membranes, the membranes were equilibrated in deionized water for 48 h, then they were removed from the water and gently blotted with filter paper to dry surface. The dimensions were measured in three directions (length, width, and thickness) to calculate the wet volume. Then, the samples were dried in a vacuum oven for 24 h at 70 °C. The ratio of volume of swollen membrane in water to the volume of dry membrane was reported as the volume swelling ratio.

The amount of acid equivalents per gram of polymer was determined as follows: First, the membrane in the acid form was immersed in 1 M NaCl solution to convert phosphoric acid to sodium form. Then, the released H^+ was back titrated with a 0.01 N NaOH solution using phenolphthalein as indicator. The IEC is the equivalents per gram of dry membrane. The IEC values of the membranes were calculated with the following equation [35]:

$$\text{IEC}\ (\text{mEq/g}) = X \times N_{\text{NaOH}}/\text{weight(polymer)} \quad (4)$$

where X is the volume of NaOH consumed and N_{NaOH} is the normality of NaOH.

Proton conductivity measurements were recorded using a Gamry (Gamry Series G 750) Potentiostat/Galvanostat/ZRA with Gamry Framework software system EIS300. The proton conductivity was measured using AC impedance spectroscopy method in the frequency range from 100 Hz to 300 kHz with potential amplitude of 10 mV. This technique allows for higher and more easily measurable resistances and a simplified setup. All measurements were performed after 100 s delay time. Membranes were fixed between two platinum electrodes in a Teflon frame (BekkTech Conductivity Clamp), and proton conductivities were measured at ambient temperature. Conductivity measurements of fully hydrated membranes were carried out with the cell immersed in distilled water. The proton conductivity, σ (S cm^{-1}), in these experiments was calculated from:

$$\sigma = \frac{L}{RWT} \quad (5)$$

Where L is the distance (cm) between two electrodes, T and W are the thickness (cm) and width of the membrane (cm), and R is the measured resistance (Ω) value. The membrane resistances were obtained from Nyquist plots by extrapolating the impedance data to the real axis on the high frequency side.

Results and discussion

FTIR analysis

The overlap of ATR-FTIR spectra of the MDP-based proton conductive membranes can be seen in Fig. 2. To make comparison, the IR spectra of all monomers were presented in the same figure. Although the ester carbonyl absorption peak of PEGDA and MDP monomers appears at 1721.50 and 1717.91 cm^{-1}, in the IR spectra of corresponding membranes (M2, M4, and M5), the C═O stretching vibrations were observed at 1723.54, 1727.51, and 1724.84 cm^{-1} respectively. As it can be seen, slight shifts observed in these peaks could be attributed to the formation of hydrogen bonding between ethereal oxygens of PEGDA and hydroxyl groups of MDP [36].

Moreover, the existence of P═O and P–O stretching bands in the spectra of membranes at 1194.15, 1011.94, and 952.10 cm^{-1} is a proof of the presence of MDP monomer in polymer chain. On the other hand, for membranes M2, M4, and M5, the peaks at 1663.77, 1656.25, and 1677.49 cm^{-1} belong to the hydrogen bonded C═O of the NVP which is caused by the interaction between NVP and MDP monomers [37]. The broadening of the C═O peak caused by the H-bonding was also observed with the increase of MDP content. In addition, the characteristic acrylate double bonds at 809.74, 1407.77, and 1618–1636 cm^{-1} was no longer detected in the spectra of UV-cured membranes. These findings also demonstrate the formation of expected structures successfully.

The determination of insoluble part of the UV-cured membranes

In order to remove unreacted and uncross-linked ingredients from UV-cured membranes, each membrane was extracted with DMAc. As shown in Table 2, the insoluble part (mass %) of UV-cured membranes was found to be 94–99 %. These results give some information about the degree of curing of the membranes and the cross-linked polymer concentration after the membrane preparation. Additionally, the disappearance of the reactive double bond upon UV irradiation can be observed in the FTIR spectrum. It is known that, prior to UV irradiation, the FTIR spectrum of the acrylated polymer membranes exhibits unsaturated double bonds at 1600–1650 cm^{-1}. Figure 3 shows that, upon UV irradiation, the double bond (C═C) at around 1650–1600 cm^{-1} disappears for the UV-cured membranes [38, 39]. Hence, the disappearance of double bonds in FTIR spectra and very high conversions prove that almost all the reactive monomers and oligomers in the feed was converted to cross-linked polymer after UV curing.

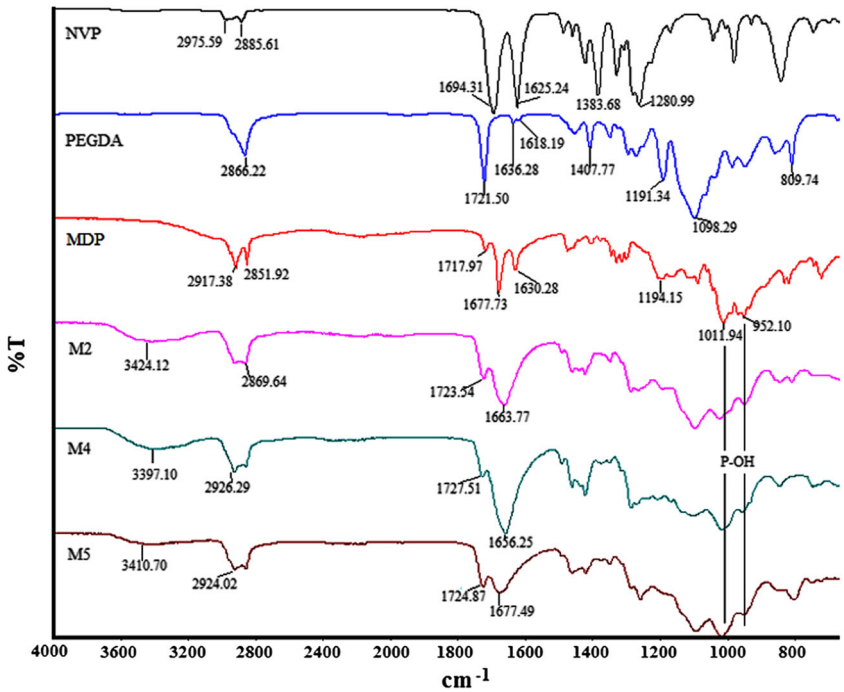

Fig. 2 FTIR spectra of PEGDA, NVP, MDP, and MDP containing UvcPMs

Thermal analysis

The thermal behavior of membranes is shown in Fig. 4. Phosphorous-containing polymers have drawn considerable attention due to their high thermal stability and proton conduction ability [11]. The initial weight loss (5 wt%) at 100–150 °C may be attributed to the moisture loss due to the hygroscopic properties of membrane components, unreacted monomers, and photoinitiator. The weight loss observed before 200 °C was attributed to the remaining nonpolimerized reactive diluent or probably due to volatilization of unreacted photoinitiator. The first irreversible weight loss occurred at 200–360 °C, depending on the content of MDP. It has been reported previously that the decomposition temperatures in the range of 250–350 °C are sufficiently high for fuel cell applications [40–42]. The char yields at 500 °C were also collected. It can be clearly seen that approximately 19 to 24 wt% of residue remains at 500 °C. These results show that proton conductive membrane is thermally stable and suitable for high temperature fuel cell applications.

Table 2 The insoluble part, soluble part, and contact angle values of UV-cured membranes

Sample	Insoluble part (%)	Soluble part (%)	Contact angel (°)
M1	99	1	86
M2	97	3	84.5
M3	97	3	80
M4	96	4	80
M5	94	6	76
M6	94	6	79

Water contact angle

Water contact angle measurement techniques are one of the most sensitive measurements for obtaining surface information from the outermost few Angstroms of solid surfaces and widely used for the surface characterization of the polymeric films [43, 44]. The surface hydrophilicity of the membranes M1–M5, as characterized by water contact angle, is summarized in Table 2. The water contact angle was found in the range of 86–76°. When the content of MDP increases in the membrane, the contact angle value decreased. This was an expected behavior because phosphate groups make more hydrophilic surface. Finally, the results indicated that the membrane hydrophilicity was improved by the introduction of the MDP.

Morphology

Morphological information was obtained by tapping mode atomic force microscopy (AFM). It is more suitable than contact mode for imaging delicate samples because of the lower lateral forces. It has been applied to many polymer systems [45, 46]. In this study, phosphoric acid groups act as the main proton carriers. By tapping mode of AFM, one can investigate the possibility of phase separation which would facilitate proton-hopping in the electrolyte. Figures 5 and 6 show the AFM topographic and phase images, respectively. Figure 5a, b displays the topographic images of samples M1 and M5.

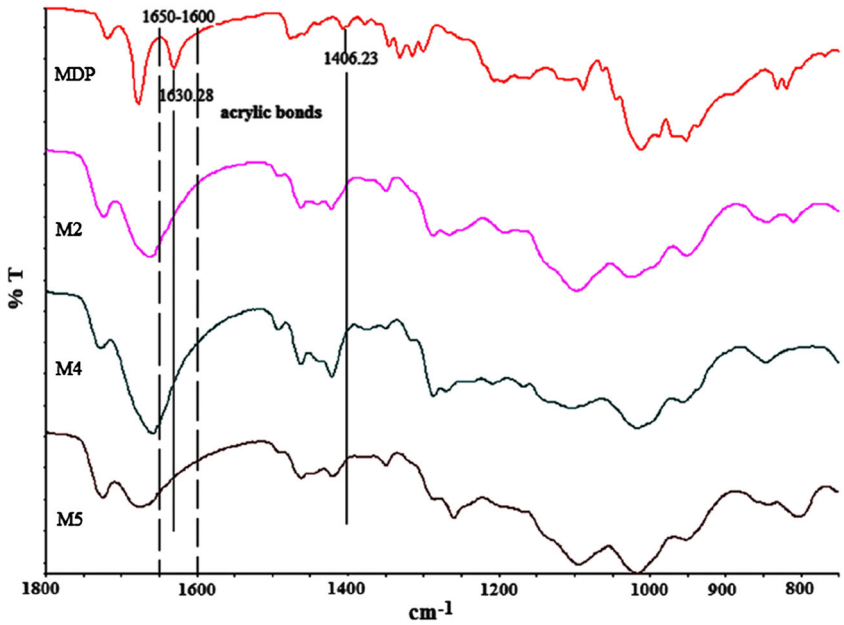

Fig. 3 FTIR spectra of MDP and MDP containing UVcPMs

The sample surfaces have different topographical features and roughness shown by the vertical profile of the membrane surface denoted by the color intensity, with bright regions being the highest points and the dark points representing the depressions and pores. When MDP amount increases from 10 wt% (M1) to 40 wt% (M5), the number of holes and grooves increased drastically as shown in Fig. 5b. Hence, M5 has more undulating structure, suggesting large hydrophilic domain size that may correlate with the surface roughness. In addition, contact angle measurements support this finding. The hydrophilic domains can be discerned by a brighter color from the hydrophobic regions of the polymer backbone. As it is obvious, sample M5 with higher MDP content has bright regions due to more ionic domains. Compared to membrane M1, the hydrophilic ionic domains in the membrane M5 become continuous to form large channels and cluster agglomeration, which is better for ion conductivity [47]. On the other hand, the "bulk-like" water in our membrane M5 which has larger domain size than Nafion® membrane causes a lower degree of water–polymer interaction, so this makes the conductivity less than Nafion [48].

The phase imaging data is shown in Fig. 6. Phase imaging in AFM is a powerful technique for producing contrast on heterogeneous samples. It refers to recording the phase shift signal in AFM. The phase signal was described as being sensitive to variations in composition, adhesion, friction, viscoelasticity as well as other factors. In these AFM phase images (Fig. 6b), the dark structures exhibited a larger phase lag and corresponded to a softer region, in which the hydrophilic phosphoric acid groups contain more fraction of water; the bright phase structure corresponds to the harder regions of the hydrophobic polymer backbone. The dark regions were not uniform but average size is about 3.5 μm for sample M5. This value is substantially larger than for Nafion® membrane [49]. As previously reported, the

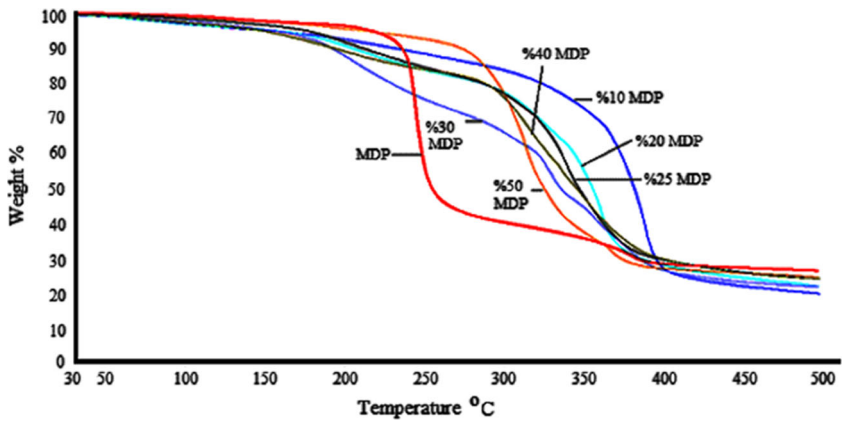

Fig. 4 TGA spectra of UVcPMs

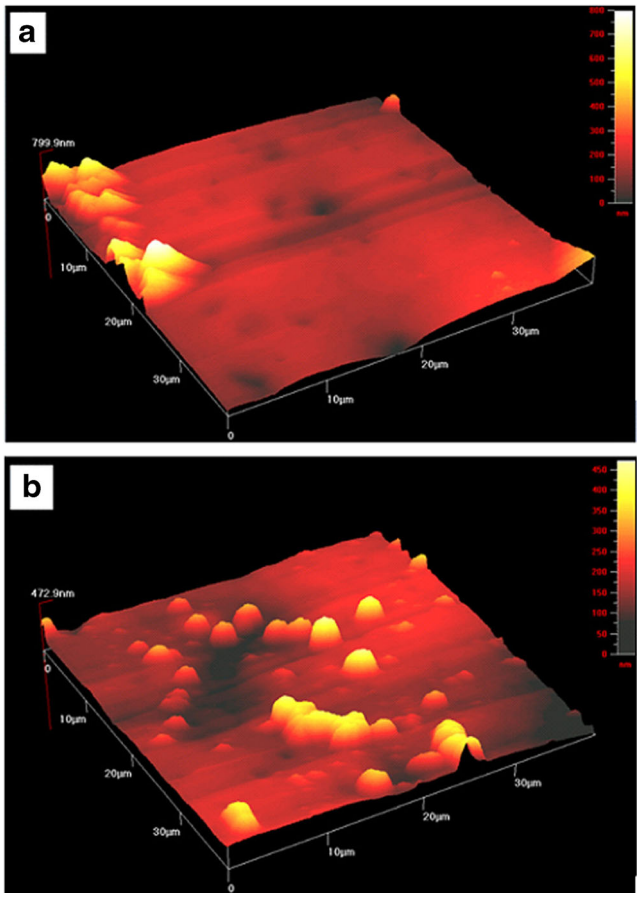

Fig. 5 Three-dimensional images of the surfaces of membranes: **a** M1 and **b** M5, respectively

properties of ion exchange membranes (IEMs) are strongly related to their internal structure which includes morphology of additives' surface, shape and size of ionic domains, and spatial distribution of ionic sites [50]. Also, ionic aggregation and phase separation are consistently found to play an important role in the proton conductivity of low IEC membranes, but a less role in high IEC membranes [47]. Compared to Nafion® membrane, the sharp increase on ionic domains was attributed to the changes in MDP particles' shape, size, and distribution [51].

Water uptake, volume swelling ratio, and ion exchange capacity

Water uptake is a vitally important issue in the development of proton-conducting membranes because the proton conduction is a water-assisted process. In general, the proton conductivity depends on the number of available acid groups and their dissociation capability in water. As can be seen from Table 1, the water uptake increases with increasing MDP and decreasing PEGDA contents. Water uptakes of UV-cured membranes changed between 36.3 and 76.1 %. Also, the effect of cross-linking on water uptake also plays a dominant role. The membrane with 40 wt% of MDP exhibited highest level of water uptake (76.1 wt%) in comparison to other phosphonated polymers reported in the literature [11, 16, 52]. The decrease in water uptake for 50 wt% of MDP-containing membranes is probably due to the formation of hydrogen bonding between amide and phosphoric acid at high concentrations and also self-hydrogen bonding ability of phosphoric acids.

The volume swelling ratio of a PEM is a widely reported volume-related parameter, but it is usually presented in the context of dimensional stability rather than in correlation with proton conductivity. It is previously reported that reduced swelling behavior of PEMs was required for improved endurance and easy control of fuel cell systems [53]. An excessive amount of ion-conducting moieties causes excessive swelling of the membrane, which leads to serious deterioration of mechanical properties and durability. In this case, it is more appropriate to use membrane swelling based on a volume. The volume swelling ratio of the UV-cured membranes was measured and found to be between 50.7 and 116.2 %, as shown in Table 1.

The ion-exchange capacity (IEC) is defined as the moles of exchangeable acidic protons per gram of dry polymer, and the

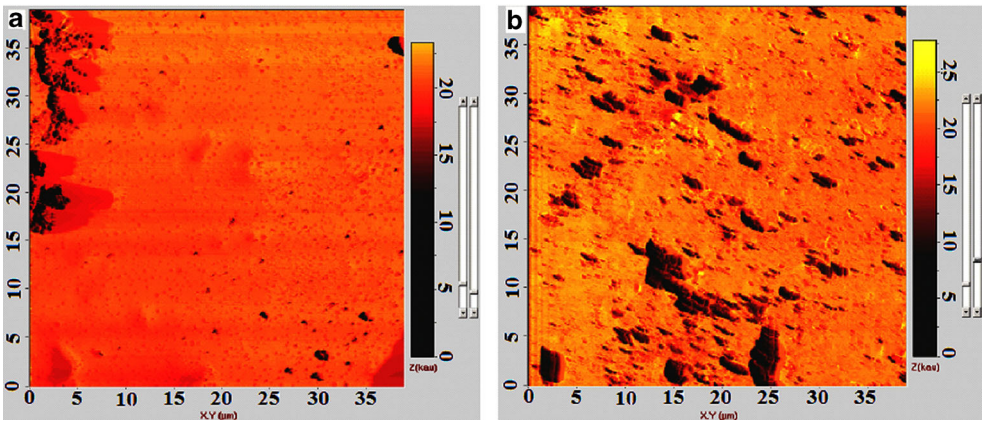

Fig. 6 Phase images of membranes **a** M1 and **b** M5. The colometric scale indicates the Z dimension. Scan rate is 1 Hz

IEC of membranes can be experimentally determined by potentiometric titration of the acid groups. The water uptake of membranes is directly related to the IEC. In the case of sulfonated membranes, where proton transport is water-assisted, a high water uptake is generally required [54]. High IECs are necessary for good proton conduction because of the high charge density of the membrane. The IEC values for MDP-based proton conductive membranes are given in Table 1. As expected, the IEC values increase with an increase in MDP monomer content. As the IEC changed from 0.27 to 0.84 meq/g, the water uptake and volume swelling ratio increased from 36.3 to 76.1 wt% and from 50.7 to 116.2 vol%, respectively. As previously reported, the decrease in IEC with increasing PEGDA content resulted in a decrease in water uptake and proton conductivity at temperatures below 70 °C [55]. Hence, related reference supports these findings.

Proton conductivity

In PEMFCs, the proton conductivity of the membrane is particularly important since it plays a significant role in the performance of the fuel cell. The proton conductivity of the membranes was measured for a wide range of compositions of MDP content using EIS as described in the experimental section; Fig. 7 shows the Nyquist diagrams used to extract the resistance values. The inset figure describes an equivalent circuit model. As can be seen, a Nyquist representation of the impedance data exhibits an arc at high frequency, a second arc at lower frequencies, and a linear portion at the lowest frequencies like many polycrystalline materials. A circuit of resistors, R, and constant phase elements, Q, has the impedance shown in Fig. 7.

The results are shown in Table 1, where it can be seen that the conductivity values are of the order of 10^{-4}–10^{-3} S cm^{-1}, and that the conductivity increases with the increase in the number of moles of MDP of the formulation. The mole ratio between MDP and NVP units has dominant influence on proton conductivity since in proton conduction, MDP and NVP may act as proton donor and acceptor, respectively, forming proton-transferring channels through the membrane. It is known that each acid can form hydrogen bonds with NVP (i.e., carbonyl of pyrrolidone ring). This hydrogen bonding between phosphoric acid group and NVP decreases the release of protons of phosphoric acid groups. Through the forming and breaking of these hydrogen bonds, protons can hop among atoms, being efficiently transported from one end of the membrane to the other [56, 57].

Also, the proton conductivities of UV-cured membranes all followed similar trends as observed for the water uptakes, volume swelling ratio, and IEC (see Table 1) except for membrane M6. As can be seen from Table 1, the lowest conductivity value obtained in the case of MDP/NVP ratio is 0.34. On the other hand, the highest proton conductivity obtained for sample M5 with MDP/NVP ratio of 1.38 as 1.11×10^{-3} Scm^{-1}. Moreover, it was supposed that swelling ratio by volume increased with the water uptake and IEC increasing for membranes M1–M5. The water uptake and swelling of the cross-linked membranes increased gradually with MDP content due to the strong hydrophilicity of the phosphoric acid groups, and the IEC also increased with increasing MDP content in soaking medium. This can be attributed to the increasing percentage ratio of phosphoric acid-containing membrane in the total structure. This is because the phosphoric acid groups on backbone can decrease the covalent nature while increasing the ionic nature of the membrane. Additionally, the contact angle results indicated that the membrane surface hydrophilicity was improved by the introduction of the MDP. Finally, swelling of the cross-linked membranes may provide space for the transport of protons and thus increase the mobility of protonic charge carriers, leading to slightly increased

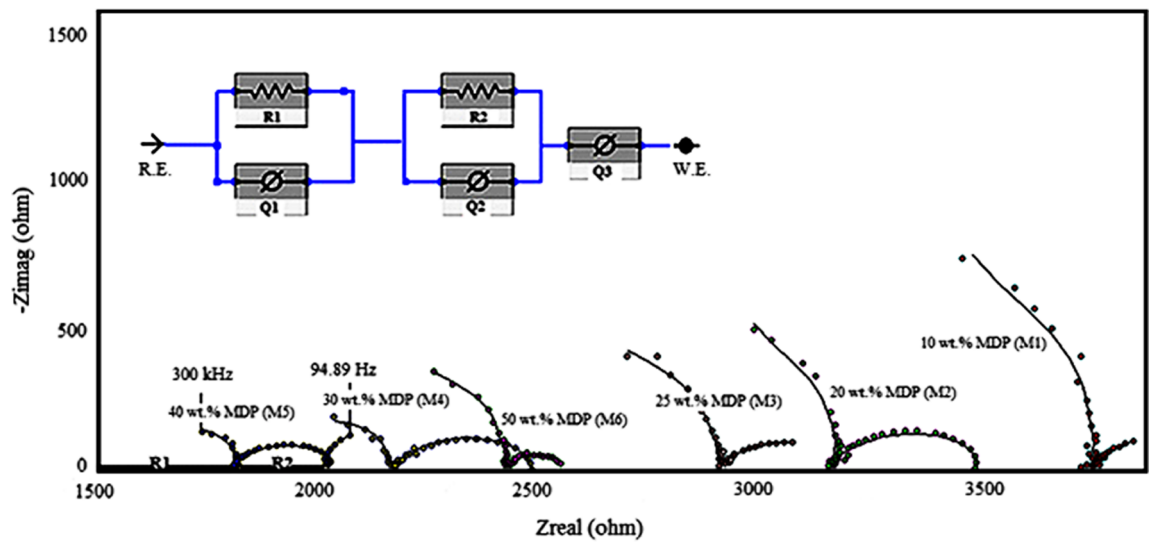

Fig. 7 A typical Nyquist plot of the MDP containing UVcPMs measured by EIS under fully hydrated conditions (frequency increases from right to left)

Table 3 Comparison of proton-conducting membranes

Additive	Proton conductivity (mS/cm)	Condition	Ref.
Poly (vinylbenzyloxy-alkyl-phosphoric acid)	0.3 at 140 °C	Anhydrous	[67]
PVPA-PVTri blend	2.1 at 100 °C	Anhydrous	[68]
H_3PO_4	62 at 150 °C	30 % R.H.	[69]
BPO_4	0.4 at room temperature	100 % R.H.	[70]
MDP	1.11 at room temperature	100 % R.H.	This work

proton conductivities. The conductivity of sample M6 is unexpectedly lower than that of M4 and M5. It is estimated that the strongest interaction between MDP and NVP will be in a molar ratio of 2:1 [58]. Therefore, sample M6 (the molar ratio of MDP:NVP is 1.72) has the strongest interaction among these series of membrane and exhibits lower proton conductivity when compared with M4 and M5 [59]. These results are consistent with the IEC, water uptakes, and volume swelling ratio of the membranes.

Moreover, the proton conductivity of membranes was at least one order lower compared to Nafion 115 and Nafion 117 measured under the similar experimental conditions. The measured conductivity of 1.2×10^{-2} and 8.0×10^{-2} Scm^{-1} for Nafion 115 and Nafion 117 membranes, respectively, in our laboratory was in the same order reported elsewhere [60–62]. As IEC increased from 0.27 to 0.84 meq/g, the volume swelling ratio increased from 50.7 to 116.2 %. Compared with the volume swelling ratio of Nafion 117 (IEC 0.91 meq/g) which is about 85 %, the swelling of sulfonated poly(vinyl fluoride) PEMs (IEC 1.5 meq/g) is about 93 % [63]. The analysis results clearly show that ionic conductivity was too low compared with previous studies. The proton conductivity of the UV-cured membranes was mainly influenced by excessive swelling. The hydrophilic character results in a relatively high water uptake and volume swelling ratio, which is detrimental to the mechanical properties of the polymer electrolytes [64]. Additionally, large water domains result in a lower degree of water–polymer interaction and more 'bulk-like' water than smaller water domains as compared to Nafion® membrane. This morphological feature has a profound impact on the macroscopic membrane properties such as mechanical stability and also related transporting proton [48]. Furthermore, it was reported that the water sorption characteristics and proton conductivities are depending not only on the water content but also on the state of water [65, 66].

The proton conductivity of phosphoric acid-based membranes in different experimental conditions can be seen in Table 3 [67–70]. From the results, it is hard to make a direct comparison of UV-cured membranes with other proton-conducting non-sulfonated membranes due to difference in temperature, polymer type, relative humidity, and method. Therefore, this side of the study can be considered as a preliminary investigation of proton-conducting properties of MDP-based UV-cured membranes.

Finally, in our study, the loosened connectivity of the proton-conducting moieties caused by the excessive swelling resulted in comparably low proton conductivities. Therefore, much more work is required in the study of these systems.

Conclusions

A series of novel polymeric proton-conducting membranes based on MDP for possible use in PEMFC were prepared by UV-curing process. These are the first PEMFCs whose monomer units contain phosphoric acid group. The membrane with 40 wt% of MDP showed high level of water uptake (76.1 wt%) and volume swelling ratio (116.2 vol%). This is attributed to the optimal concentration of phosphoric acid moieties. Above this concentration, specific interactions dominate followed by a decreased swelling. At the optimal phosphoric acid content, membrane with 40 wt% of MDP reached a conductivity of 1.11 $mScm^{-1}$ and IEC value of 0.84 meq/g at room temperature under fully hydrated conditions. This result clearly indicates the dependence of the proton conductivity on two factors. The first is the local concentration of the acidic sites (IEC) available in the hydrophilic domain, and the second factor is its ability of forming hydrogen bonds with the surrounding molecules which mainly contribute to the proton-hopping mechanism. Surely, ionic conductivity was too low compared with previous studies for both of sulfonated and phosphonated electrolytes, but also we proposed a new type of electrolyte which can be obtained by simple, cheap and fast preparation method. Furthermore, the synthesized membranes possess thermal stability up to 200 °C.

Acknowledgments This work was supported by Marmara University, Commission of Scientific Research Project under grant FEN-E-090113-0006.

References

1. Savadoga O (1998) Emerging membranes for electrochemical systems: (I) solid polymer electrolyte membranes for fuel cell systems. J New Mater Electrochem Syst 1:47–66

2. Higashihara T, Matsumoto K, Ueda M (2009) Sulfonated aromatic hydrocarbon polymers as proton exchange membranes for fuel cells. Polymer 50:5341–5357
3. Ghassemi H, McGrath JE (2004) Synthesis and properties of new sulfonated poly(p-phenylene) derivatives for proton exchange membranes. Polymer 45:5847–5854
4. Nakabayashi K, Higashihara T, Ueda M (2010) Highly sulfonated multiblock copoly(ether sulfone)s for fuel cell membranes. J Polym Sci Part A: Polym Chem 48:2757–2764
5. Lafitte B, Jannasch P (2007) Polysulfone ionomers functionalized with benzoyl (difluoromethylenephosphonic acid) side chains for proton-conducting fuel-cell membranes. J Polym Sci Part A: Polym Chem 45:269–283
6. Schuster M, Rager T, Noda A (2005) About the choice of the protogenic group in PEM separator materials for intermediate temperature, low humidity operation: a critical comparison of sulfonic acid, phosphonic acid and imidazole functionalized model compounds. Fuel Cells 5:355–365
7. Paddison SJ, Kreuer KD, Maier J (2006) About choice of the protogenic group in polymer electrolyte membranes: Ab initio modelling of sulfonic acid, phosphonic acid, and imidazole functionalized alkanes. Phys Chem Chem Phys 8:4530–4542
8. Kreuer KD, Rabenau A, Weppner W (1982) Vehikel-Mechanismus, ein neues Modell zur Deutung der Leitfähigkeit schneller Protonenleite. Angew Chem 94:159–230
9. Steininger H, Schuster M, Kreuer KD et al (2007) Intermediate temperature proton conductors for PEM fuel cells based on phosphonic acid as protogenic group: a progress report. Phys Chem Chem Phys 9:1764–1773
10. Parvole J, Jannasch P (2007) In: Zhao TS, Kreuer KD, Nguyen TV (eds) Advances in fuel cells. Elsevier, New York, pp 120–185
11. Parvole J, Jannasch P (2008) Polysulfones grafted with poly(vinylphosphonic acid) for highly proton conducting fuel cell membranes in the hydrated and nominally dry state. Macromolecules 41:3893–3903
12. Steele BCH, Heinzel A (2001) Materials for fuel cell technologies. Nature 414:345–352
13. Rikukawa M, Sanui K (2000) Proton-conducting polymer electrolyte membranes based on hydrocarbon polymers. Prog Polym Sci 25:1463–1502
14. Bock T, Möhwald H, Mülhaupt R (2007) Arylphosphonic acid-functionalized polyelectrolytes as fuel cell membrane material. Macromol Chem Phys 208:1324–1340
15. Atanasov V, Kerres J (2011) Highly phosphonated polypentafluorostyrene. Macromolecules 44:6416–6423
16. Shao Z, Sannigrahi A, Jannasch P (2013) Poly(tetrafluorostyrenephosphonicacid)-polysulfone block copolymers and membranes. J Polym Sci Part A: Polym Chem 51: 4657–4666
17. Zeng J, He B, Lamb K et al (2013) Anhydrous phosphoric acid functionalized sintered mesoporous silica nanocomposite proton exchange membranes for fuel cells. ACS Appl Mater Interfaces 5: 11240–11248
18. Grondin J, Rodriguez D, Lassegues JC (1995) Proton conducting polymer electrolyte—the Nylon 6-10/H_3PO_4 blends. Solid State Ionics 77:70–75
19. Rodriguez D, Jegat C, Trinquet O et al (1993) Proton conduction in poly (acryl amide)-acid blends. Solid State Ionics 61:195–202
20. Petty-Weeks S, Zupancic JJ, Swedo JR (1988) Proton conducting interpenetrating polymer networks. Solid State Ionics 31:117–125
21. Tanaka R, Yamamoto H, Shono A (2000) Proton conducting behavior in non-crosslinked and crosslinked polyethyleneimine with excess phosphoric acid. Electrochim Acta 45:1385–1389
22. He R, Li Q, Xiao G et al (2003) Proton conductivity of phosphoric acid doped polybenzimizadole and its composites with inorganic proton conductors. J Membr Sci 226:169–184
23. Honma I, Takeda Y, Bae JM (1999) Protonic conducting properties of sol-gel derived organic / inorganic nanocomposite membranes doped with acidic functional molecules. Solid State Ionics 120: 255–264
24. Honma I, Nomura S, Nakajima H (2001) Protonic conducting organic/inorganic nanocomposites for polymer electrolyte membrane. J Membr Sci 185:83–94
25. Nakabayashi N (1985) Bonding of restorative materials to dentin: the present status in Japan. Int Dent J 35:145–154
26. Kadoma Y (2003) Chemical structures of adhesion promoting monomers for precious metals and their bond strengths to dental metals. Dent Mater J 22:343–358
27. Yoshida Y, Nagakane K, Fujuda R et al (2004) Comparative study on adhesive performance of functional monomer. J Dent Res 83: 454–458
28. Fujisawa S, Kadoma Y, Komoda Y (1991) HPLC separation of methacryloyloxy dihydrogen phosphate from dental bonding agents. Jap J Dent Mater 10:30–34
29. Bayramoglu G, Kahraman MV, Kayaman-Apohan N et al (2007) Synthesis and characterization of UV-curable dual hybrid oligomers based on epoxy acrylate containing pendant alkoxysilane groups. Polym Adv Technol 17:1–7
30. Cakmakci E, Mulazim Y, Kahraman MV (2013) UV-curable fluorine-containing hybrid coatings via thiol-ene 'click' reaction and an in situ sol-gel method. Polym Bull 70:1037–1048
31. Chen MH, Chen CR, Hsu SH et al (2006) Low shrinkage light curable nanocomposite for dental restorative material. Dent Mater 22:138–145
32. El-Molla MM (2007) Synthesis of polyurethane acrylate oligomers as aqueous UV-curable binder for inks of ink jet in textile printing and pigment dyeing. Dyes Pigments 74:371–379
33. Gurtekin M, Kayaman-Apohan N, Kahraman MV et al (2009) UV curable sulfonated hybrid materials and their performance as proton exchange membranes. React Funct Polym 69:698–704
34. Akdemir ZS, Akcakaya H, Kahraman MV et al (2008) Photopolymerized injectable RGD-modified fumarated poly(ethylene glycol) diglycidyl ether hydrogels for cell growth. Macromol Biosci 8:852–862
35. Goh YT, Patel R, Im SJ et al (2009) Synthesis and characterization of poly(ether sulfone) grafted poly(styrene sulfonic acid) for proton conducting membranes. Korean J Chem Eng 26:518–522
36. Preari M, Spinde K, Lazic J et al (2014) Bioinspired insights into silicic acid stabilization mechanisms: the dominant role of polyethylene glycol-induced hydrogen bonding. J Am Chem Soc 136(11): 4236–4244
37. Kuo S-W, Shih C-C, Shieh J-S et al (2004) Specific interactions in miscible polymer blends of poly(2-hydroxypropyl methacrylate) with polyvinylpyrrolidone. Polym Int 53:218–224
38. Ali MA, Ooi TL, Salmiah A et al (2001) New polyester acrylate resins from palm oil for wood coating application. J Appl Polym Sci 79:2156–2163
39. Flatten A, Bryhni EA, Kohler A et al (2005) Determination of C22: 5 and C22:6 marine fatty acids in pork fat with Fourier transform midinfrared spectroscopy. Meat Sci 69:433–440
40. Fukuzaki N, Nakabayashi K, Nakazawa S et al (2011) Highly phosphonated poly(N-phenylacrylamide) for proton exchange membranes. J Polym Sci: Part A: Polym Chem 49:93–100
41. Wang F, Hickner M, Kim YS et al (2002) Direct polymerization of sulfonated poly(arylene ether sulfone) random (statistical) copolymers: candidates for new proton exchange membranes. J Membr Sci 197:231–242
42. Karlsson LE, Jannasch P (2004) Polysulfone ionomers for proton-conducting fuel cell membranes: sulfoalkylated polysulfones. J Membr Sci 230:61–70

43. Andrade JD, Smith LM, Gregonis DE (1985) The contact angle and interface energetics. In: Andrade JD (ed) Surface and interfacial aspects of biomedical polymers. Plenum Press, N.Y
44. Arnett NY, Harrison WL, Badami AS et al (2007) Hydrocarbon and partially fluorinated sulfonated copolymer blends as functional membranes for proton exchange membrane fuel cells. J Power Sources 172:20–29
45. Ratner BD, Tsukruk VV (1998) Scanning probe microscopy in polymers. ACS Symposium, vol 694. American Chemical Society, Washington, DC
46. James PJ, McMaster TJ, Newton JM et al (2000) In situ rehydration of perfluorosulphonate ion-exchange membrane studied by AFM. Polymer 41:4223–4231
47. Yang Y, Holdcroft S (2005) Synthetic strategies for controlling the morphology of proton conducting polymer membranes. Fuel Cells 5:171–186
48. Benoit Lafitte, Proton-conducting sulfonated and phosphonated polymers and fuel cell membranes by chemical modification of polysulfones, Lund University (2007) Doctor of Philosophy of Engineering Thesis
49. Smitha B, Sridhar S, Khan AA (2005) Solid polymer electrolyte membranes for fuel cell applications. J Membr Science 259:10–26
50. Fujimura M, Hashimoto T, Kawai H (1981) Small-angle X-ray scattering study of perfluorinated ionomer membranes. 1. Origin of two scattering maxima. Macromolecules 14:1309–1315
51. Yun S, Parrondo J, Zhang F et al (2014) Microstructure-property relationships in sulfonated polyether ether ketone/silsesquioxane composite membranes for direct methanol fuel cells. J Electrochem Soc 161:815–822
52. Steininger H, Schuster M, Kreuer KD et al (2006) Intermediate temperature proton conductors based on phosphonic acid functionalized oligosiloxanes. Solid State Ionics 177:2457–2462
53. Wang H, Badami A, Roy A et al (2006) Multiblock copolymers of poly(2,5-benzophenone) and disulfonated poly(arylene ether sulfone) for proton-exchange membranes I. Synthesis and characterization. J Polym Sci Part A: Polym Chem 45:284–294
54. Peron J, Ruiz E, Jones DJ et al (2008) Solution sulfonation of a novel polybenzimidazole A proton electrolyte for fuel cell application. J Membr Sci 314:247–256
55. Lee S, Jang W, Choi S et al (2007) Sulfonated polyimide and poly (ethylene glycol) diacrylate based semi-interpenetrating polymer network membranes for fuel cells. J Appl Polym Sci 104:2965–2972
56. Lee YJ, Murakhtina T, Sebastiani D et al (2007) H Solid-state NMR of mobile protons: it is not always the simple way. J Am Chem Soc 129:12406–12407
57. Jiang F, Kaltbeitzel A, Meyer WH et al (2008) Proton-conducting polymers via atom transfer radical polymerization of diisopropyl-p-vinylbenzyl phosphonate and 4-vinylpyridine. Macromolecules 41: 3081–3085
58. Pu H, Luo H, Wan D (2013) Synthesis and properties of amphoteric copolymer of 5-vinyltetrazole and vinylbenzyl phosphonic acid. J Polym Sci Part A: Polym Chem 51:3486–3493
59. Wang P, Liu B, Li L et al (2008) Hydrogen bonding interactions in miscible blends of poly(hydroxyether ester)s with poly(n-vinyl pyrrolidone). J Macromol Sci Part B: Phys 47(4):800–817
60. Li L, Zhang J, Wang Y (2003) Sulfonated poly(ether ether ketone) membranes for direct methanol fuel cell. J Membr Sci 226:159–167
61. Edmondson CA, Stallworth PE, Wintersgill MC et al (1998) Electrical conductivity and NMR studies of methanol/water mixtures in Nafion membranes. Electrochim Acta 43:1295–1299
62. Kim DS, Park HB, Rhim JW et al (2005) Proton conductivity and methanol transport behavior of cross-linked PVA/PAA/Silica hybrid membranes. Solid State Ionics 176(1):117–126
63. Vie P, Paronen M, Stomgard M et al (2002) Fuel cell performance of proton irradiated and subsequently sulfonated poly(vinyl fluoride) membranes. J Membr Sci 204(1-2):295–301
64. Zhilian Zhou, Novel polymer electrolyte membranes for fuel cell applications, Department of Chemistry Chapel Hill (2006) University of North Carolina, degree of Doctor of Philosophy
65. Liu C-P, Dai C-A, Chao C-Y et al (2014) Novel proton exchange membrane based on crosslinked poly(vinyl alcohol) for direct methanol fuel cells. J Power Sources 249(3):285–298
66. Dai C-A, Liu C-P, Lee Y-H et al (2008) Fabrication of novel proton exchange membranes for DMFC via UV curing. J Power Sources 177(2):262–272
67. Lee S-II, Yoon K-H, Song M et al (2012) Structure and properties of polymer electrolyte membranes containing phosphonic acids and anhydrous fuel cells. Chem Mater 24(1):115–122
68. Yue B, Yan L, Han S et al (2013) Proton transport pathways in an acid-base complex consisting of a phosphonic acid group and a 1,2, 3-triazolyl group. J Phys Chem B 117(26):7941–7949
69. Asensio JA, Borros S, Romero G (2004) Polymer electrolyte fuel cells based on phosphoric acid-impregnated poly(2,5-benzimidazole) membranes. J Electrochem Soc 151(2):A304–A310
70. Çakmakçı E, Güngör A (2013) Preparation and characterization of flame retardant and proton conducting boron phosphate/polyimide composites. Polym Degrad Stab 98:927–933